# Single AAV-mediated scarless genome editing in dysfunctional retinal neurons mediates robust visual restoration in mice

Short title: Single AAV scarless genome editing

Koji M Nishiguchi,[1,2†*] Kosuke Fujita,[3†] Shota Katayama,[1] Toru Nakazawa[1,2,3*]

[1] Department of Advanced Ophthalmic Medicine, Tohoku University Graduate School of Medicine, Sendai 980-8574, Japan

[2] Department of Ophthalmology, Tohoku University Graduate School of Medicine, Sendai 980-8574, Japan

[3] Department of Ophthalmic Imaging and Information Analytics, Tohoku University Graduate School of Medicine, Sendai 980-8574, Japan

[†] These authors contributed equally to the work.

[*] Corresponding authors. Tel: +81-22-717-7294

Koji M Nishiguchi, E-mail: nishiguchi@oph.med.tohoku.ac.jp

Toru Nakazawa, E-mail: ntoru@oph.med.tohoku.ac.jp

**The most versatile treatment for inherited disorders is to precisely replace a mutated sequence with its wildtype counterpart, thereby *"normalizing"* the genome. We developed a single AAV platform that allows this in retinal neurons with combined CRISPR-Cas9 and micro-homology-mediated end-joining. In blind mice, the platform rescued ~10% of the retinal neurons, resulting in an incredible ~10,000-fold improvement in light sensitivity, equivalent to the restoration mediated by conventional gene augmentation therapy.**

Gene supplementation of wildtype copies of functionally defective genes (gene augmentation) mediated by adeno associated virus (AAV) have shown remarkable success in clinical trials for inherited neural disorders. [1,2] However, its application is restricted to limited genes within the capacity (~5,000 bps) of AAV.[3] CRISPR-Cas9-mediated allele knock-out based on error-prone non-homologous end joining (NHEJ) can correct gain-of-function mutations with AAV.[4-7] However, many loss-of-function mutations in larger genes still require local replacement with a wildtype sequence (scarless genome editing).

Here, we used micro-homology-mediated end-joining (MMEJ) to integrate a donor template with micro-homology arms of 20 bp[8] as the basis for a new single-AAV platform

for scarless genome editing. First, we generated mutants of the preexisting retina-specific promoters and conducted *in vivo* AAV reporter assays (Fig. S1a-c, Table S1). The smallest promoter that maintained neural retina-specific transcription was a 93-bp mutant GRK1 promoter that allowed reporter expression in 65.5% of the photoreceptors (Fig. S1b-e). This was used to drive SaCas9 (3.2 Kb) expression.

We tested our single-AAV vector platform in *Gnat1*$^{IRD2/IRD2}$/*Pde6c*$^{cpfl1/cpfl1}$ mice (double-mutant mice); the *Gnat1* and *Pde6c* defects caused functional lack of rod and cone photoreceptors,[9] respectively. The mice were essentially blind from birth and thus allowed clear delineation of therapeutic effects.[10] We used our platform to correct *IRD2* mutations in *Gnat1*; these mutations constitute a homozygous 59-bp deletion in intron 4, preventing protein expression in the rod photoreceptors[11], which comprise ~75% of the murine retinal cells.[12] Six guide RNAs (gRNAs) designed flanking the mutation were assessed with a T7 Endonuclease 1 (T7E1) assay (Fig. S2). A gRNA pair (1+4) that excised the mutation most efficiently was selected. The constructed single-AAV vector (Fig. 1a) was then injected sub-retinally in 6-month-old double-mutant mice. Five weeks later, histology showed scattered GNAT1-positive photoreceptors, indicating successful genome editing (Fig. 1b). T7E1 assay (Fig. 1c) and RT-PCR (Fig. 1d) of the whole retina revealed absolute editing efficacies of 8.6% and 12.7% among the rod photoceptors, respectively. Furthermore,

electroretinogram (ERG), which reflects the number of functional photoreceptors, revealed 6-Hz flicker responses, averaging 11.4% of the control mice (Fig. 1e). These results are consistent with a ~10% rescue of the rod photoreceptors by genome editing.

Next, light sensitivity in the visual cortex was assessed with flash visually evoked potentials (fVEPs). Surprisingly, cortical responses contralateral to the treated eye revealed a ~10,000-fold (range: 1,000 – 100,000-fold) improvement in light sensitivity, equivalent to gene augmentation in ~70% of the photoreceptors (Fig. 1f and g, S1e, S3).[10] This was reflected by changes in light-induced behavior (fear conditioning, Fig. 1h). Furthermore, contralateral cortical responses to phase-reversal gratings, i.e., the pattern VEP (pVEP), were detected in higher resolution gratings with larger amplitudes following the treatment, indicating improved visual acuity (Fig. 1i). Threshold assessment by measuring optokinetic responses to rotating gratings showed visual acuity restoration in the treated mice to 59.1% of the control mice. (Fig. 1j).

On-target analysis of retinal genomic DNA with sequencing revealed an absolute indel rate of 36.4% (Table S3), somewhat higher than previous reports[13,14]. Three sites predicted to have the highest off-target probabilities for each gRNA showed no detectable mutation events in the retinal genomic DNA (Fig. S4) by the T7E1 assay. Further sequencing of these sites found no mutations (Fig. S4).

We also used our AAV vector to treat 2-month-old *Gnat1*$^{IRD2/IRD2}$ mice, which retain cone function and serve as a model of human retinal dystrophy.[15] In the early course of the disease, patients suffer from severe loss of light sensitivity with preserved visual acuity. [15] A histological analysis showed scattered GNAT1-postive photoreceptors in the treated mice (Fig. 2a). T7E1 assay and RT-PCR measured absolute genome editing efficacy at 7.5% and 7.2%, respectively (Fig. S5a,b). fVEP showed a ~1,000-fold increase in light sensitivity (Fig. 2b). This was confirmed behaviorally with fear conditioning (Fig. 2c). However, the improvement in retinal function could not be isolated from preexisting cone function with ERG and visual acuity remained unchanged with pVEP, or OKR (Fig. S5c-e). These results show that our platform had therapeutic effects also in a human disease model.

This study shows that scarless genome editing allows a striking improvement in light sensitivity, the major biomarker adopted in the seminal clinical trials for retinal dystrophy.[2] Moreover, the effect was equivalent to that of conventional gene augmentation therapy[10], a platform that is already in clinical use,[16] and was achieved with a single AAV vector. This is a major step forward from the dual vector system used in previous studies on donor-based *in vivo* genome editing in post-mitotic cells, which generally yielded an absolute editing efficiency of less than ~5%[13,14,17,18], compared to ~10% shown herein. Additional important advantages of scarless genome editing include physiological and

uniform expression of the target gene, neither of which is possible with gene augmentation. This may be critically important to avoid dose-related toxicity caused by both gene over-expression[19] and under-expression[20], especially during long-term treatment in humans.

As a proof of concept, our platform for single AAV-mediated scarless genome editing demonstrates amelioration of key features of dysfunctional neurons. This paves the way to treat inherited neural disorders caused by loss-of-function mutations in larger genes, for which conventional gene augmentation therapy or NHEJ-based genome editing strategies are not currently feasible.

**Reference**

1. Mendell, J.R.*, et al. N. Engl. J. Med.* **377**, 1713-1722 (2017).
2. Cideciyan, A.V. *Prog. Retin. Eye Res.* **29**, 398-427 (2010).
3. Wu, Z., Yang, H. & Colosi, P. *Mol. Ther.* **18**, 80-86 (2010).
4. Tsai, Y.T.*, et al. Ophthalmology* **125**, 1421-1430 (2018).
5. Yang, S.*, et al. J. Clin. Invest.* **127**, 2719-2724 (2017).
6. Gaj, T.*, et al. Science advances* **3**, eaar3952 (2017).
7. Li, P.*, et al. The CRISPR Journal* **1**, 55-64 (2018).
8. Nakade, S.*, et al. Nature communications* **5**, 5560 (2014).

9. Lamb, T.D. *Prog. Retin. Eye Res.* **36**, 52-119 (2013).

10. Nishiguchi, K.M.*, et al. Mol. Ther.* **26**, 2397-2406 (2018).

11. Miyamoto, M.*, et al. Exp. Eye Res.* **90**, 63-69 (2010).

12. Jeon, C.J., Strettoi, E. & Masland, R.H. *J. Neurosci.* **18**, 8936-8946 (1998).

13. Yin, H.*, et al. Nat. Biotechnol.* **34**, 328 (2016).

14. Yang, Y.*, et al. Nat. Biotechnol.* **34**, 334 (2016).

15. Carrigan, M.*, et al. Br. J. Ophthalmol.* **100**, 495-500 (2016).

16. Kaltenboeck, A. & Bach, P.B. *JAMA* (2018).

17. Suzuki, K.*, et al. Nature* **540**, 144-149 (2016).

18. Yin, H.*, et al. Nat. Biotechnol.* **32**, 551 (2014).

19. Tan, E.*, et al. Invest. Ophthalmol. Vis. Sci.* **42**, 589-600 (2001).

20. Verbakel, SK., *et al. Invest. Ophthalmol. Vis. Sci.* (2019) *in press*.

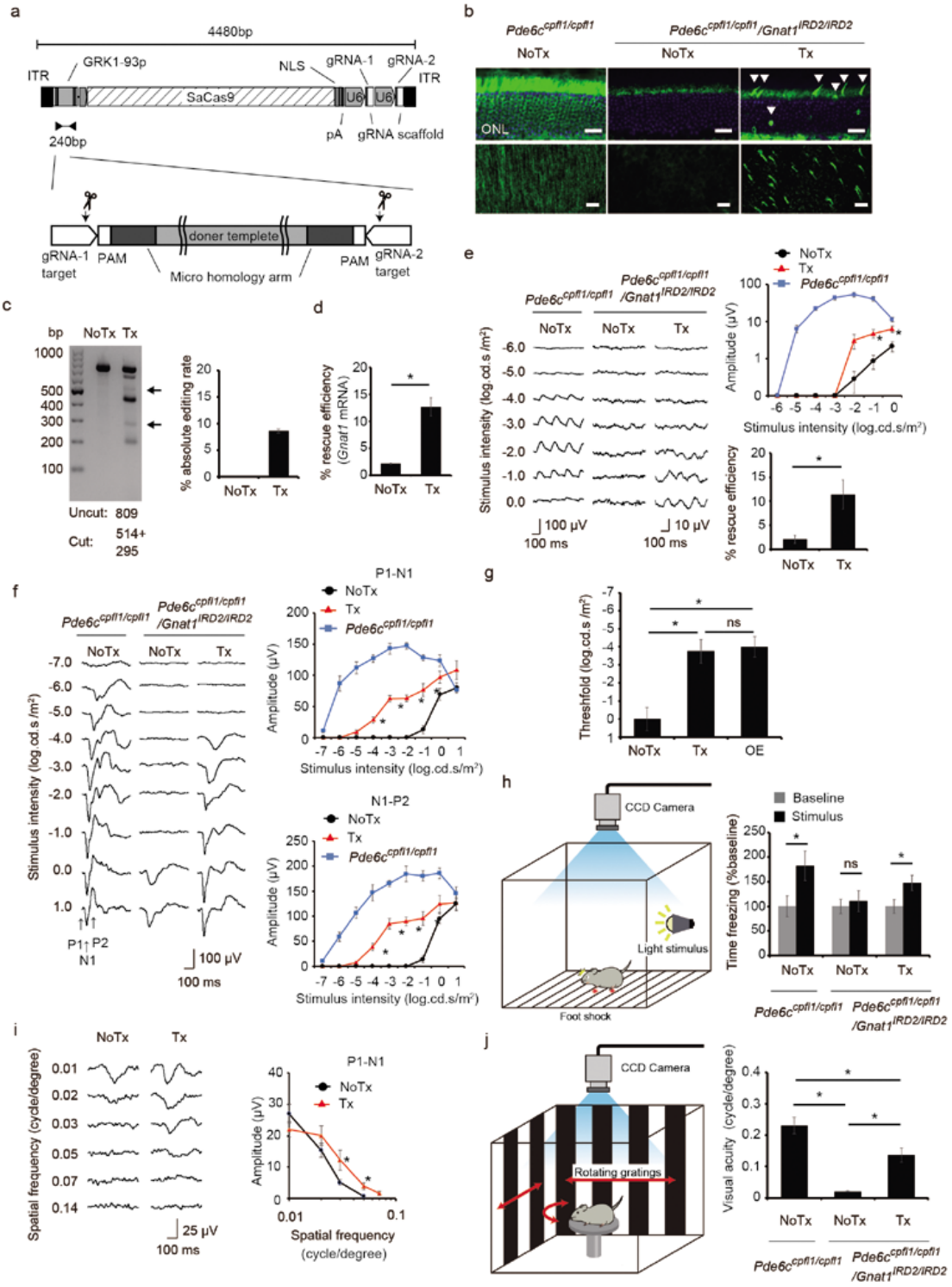


**Fig 1. *In vivo* scarless genome editing and visual restoration in blind mice**

**a.** Design of the all-in-one vector with an enlarged map of the donor sequence. ITR, inverted terminal repeat; NLS, nuclear localizing signal; pA, ploy A; PAM, protospacer adjacent motif. **b.** GNAT1-positive photoreceptors (arrowhead) following genome editing in a retinal section (top) and a flat mount (bottom). Scale bar: 20 µm. **c.** T7E1 assay. Representative image (left) and stats (right, N = 4). Arrows: size of cleaved fragments (also indicated below). **d.** RT-PCR (N = 4). **e.** 6-Hz flicker ERGs in treated and untreated eyes of the same *Pde6c*$^{cpfl1/cpfl1}$*Gnat1*$^{IRD2/IRD2}$ mice (N = 6) and control *Pde6c*$^{cpfl1/cpfl1}$ mice (N = 5). **f.** fVEPs recorded from contralateral visual cortices of treated and untreated eyes of *Pde6c*$^{cpfl1/cpfl1}$*Gnat1*$^{IRD2/IRD2}$ mice (N = 9) and control *Pde6c*$^{cpfl1/cpfl1}$ mice (N = 5). **g.** Thresholds of fVEP. *Pde6c*$^{cpfl1/cpfl1}$*Gnat1*$^{IRD2/IRD2}$ mice were treated either with genome editing (N = 9) or *GNAT1* over-expression (OE, N = 6) or left untreated (N =9). **h.** Fear conditioning test. Freezing time before (Baseline) and during (Stimulus) presentation of fear-conditioned light cue (N = 6 each). **i.** pVEPs from treated (N = 9) and untreated (N = 5) *Pde6c*$^{cpfl1/cpfl1}$*Gnat1*$^{IRD2/IRD2}$ mice. **j.** Optokinetic response in the treated (N = 10) and untreated (N = 4) *Pde6c*$^{cpfl1/cpfl1}$*Gnat1*$^{IRD2/IRD2}$ mice and untreated *Pde6c*$^{cpfl1/cpfl1}$ mice (N = 6). Data represent the mean ± S.E.M.; *P < 0.05; Tx, treated; NoTx untreated; OE, over-expression; nd, non-detectable; ns, not significant.

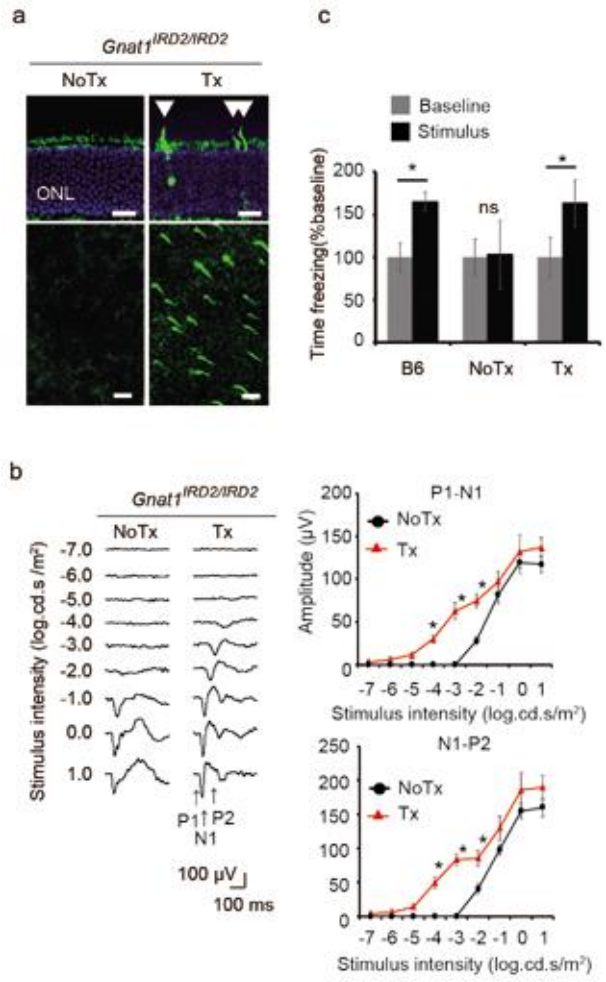


**Fig 2. In vivo scarless genome editing in a mouse model of retinal degeneration**

**a.** GNAT1-positive photoreceptors (arrowhead) following treatment of *Gnat1*$^{IRD2/IRD2}$ mice shown in a retinal section (top) and a flatmount (bottom). Scale bar: 20 µm. **b.** fVEPs recorded from contralateral visual cortices in treated and untreated eyes of the same mice. (N = 7). **c.** Fear conditioning test, showing freezing time before (Baseline) and during (Stimulus) presentation of fear-conditioned light cue. Treated (Tx, N = 7) and untreated (NoTx, N = 6) *Gnat1*$^{IRD2/IRD2}$ mice and CL57B6 mice (B6, N = 6). Data represent the mean ± S.E.M.; *P < 0.05; ONL, outer nuclear layer. ns, not significant.

## Acknowledgements

We thank Ms Misane Uchiike for her help with the experiments. This work was supported in part by the Japan Agency for Medical Research and Development (KMN, 18ek0109213h0002). The manuscript was edited by a professional English editing service (Mr. Tim Hilts).

## Author contributions

KMN conceived and designed the experiments. KMN and KF performed the experiments and analyzed the data. SK helped in vitro experiments and gave critical advice. KMN and TN wrote the manuscript and obtained the funding.

## Competing financial interests

KMN, KF, and TN are listed as inventors in a patent application related to this work. The Departments of Advanced Ophthalmic Medicine and Ophthalmic Imaging and Information Analytics are endowed departments, supported by an unrestricted grant from Senju Pharmaceutical Co. (Osaka, Japan) and Topcon Co. Ltd. (Tokyo, Japan), respectively. These funders had no role in the study design, data collection and analysis, decision to

publish, or preparation of the manuscript.

## Data availability

The datasets generated during and/or analyzed during the current study are available from the corresponding author on reasonable request.